An Assessment of the Surface Turbulent Heat Fluxes from the NCEP–NCAR Reanalysis over the Western Boundary Currents

G. W. K. MOORE

Department of Physics, University of Toronto, Toronto, Ontario, Canada

I. A. RENFREW

British Antarctic Survey, Cambridge, United Kingdom

(Manuscript received 28 September, in final form 23 January 2002)

ABSTRACT

With the completion of the NCEP–NCAR and ECMWF reanalyses there are now global representations of air–sea surface heat fluxes with sufficient spatial and temporal resolution to be useful in characterizing the air–sea interaction associated with individual weather systems, as well as in developing global-scale oceanic heat and moisture budgets. However, these fluxes are strongly dependent on the numerical models used, and, as a result, there is a clear need to validate them against observations. Accurate air–sea heat flux estimates require a realistic representation of the atmospheric boundary layer, and the implementation of an appropriate surface flux parameterization. Previous work at high latitudes has highlighted the shortcomings of the surface turbulent heat flux parameterization used in the NCEP–NCAR reanalysis during high wind speed conditions, especially when combined with large air–sea temperature differences. Here the authors extend this result through an examination of the air–sea heat fluxes over the western boundary currents of the North Atlantic and North Pacific Oceans. These are also regions where large transfers of heat and moisture from the ocean to the atmosphere take place. A comparison with in situ data shows that the surface layer meteorological fields are reasonably well represented in the NCEP–NCAR reanalysis, but the turbulent heat flux fields contain significant systematic errors. It is argued that these errors are associated with shortcomings in the bulk flux algorithm employed in the reanalysis. Using the NCEP–NCAR reanalysis surface layer meteorological fields and a more appropriate bulk flux algorithm, ''adjusted'' fields for the sensible and latent heat fluxes are presented that more accurately represent the air–sea exchange of heat and moisture over the western boundary currents.

1. Introduction

The exchange of heat and freshwater across the air–sea interface is an important coupling between the atmosphere and ocean. The energy transferred by these fluxes plays a crucial role, on a variety of spatial and temporal scales, in the atmospheric and oceanic circulation. It is through these fluxes that the atmosphere plays a key part in the water mass transformations that are an integral component of the thermohaline circulation of the ocean (Bunker and Worthington 1976; Schmitz and McCartney 1993; Lab Sea Group 1998). Likewise, numerous feedbacks, whereby the ocean has an important influence on the atmospheric circulation, are enabled by these air–sea fluxes. For example, the modification of the atmospheric boundary layer has been shown to accelerate the deepening rate of synoptic and mesoscale cyclones (Rasmussen 1989; Kuo et al. 1991). Indeed, it has been suggested that improvements in medium-range forecasts will only be attained once a better representation of air–sea fluxes is implemented in numerical weather prediction models (Brown 1990).

Following the completion of the first generation of meteorological reanalyses, by both the National Centers for Environmental Prediction–National Center for Atmospheric Research (NCEP–NCAR) and the European Centre for Medium-Range Weather Forecast (ECMWF), there exists the possibility of using the surface heat flux fields from them to generate basin-scale estimates of the air–sea fluxes (e.g., Garnier et al. 2000; WGASF 2001). Furthermore, the availability of the reanalysis fields (every 6 h) allows for their use in characterizing the air–sea interaction associated with synoptic-scale weather systems (Moore et al. 2002). However, caution must be exercised as these flux fields are, by necessity, forecasts and indeed are strongly dependent on the parameterizations employed in the numerical weather prediction model used in the reanalysis (e.g., Kalnay et al. 1996). As a result, there is a clear need to validate them against observations so as to increase our confidence in the

Corresponding author address: Dr. G. W. K. Moore, Department of Physics, University of Toronto, 60 St. George Street, Toronto, ON M5S 1A7, Canada.
E-mail: moore@atmosp.physics.utoronto.ca

fidelity of the modeled heat and moisture fluxes. Any such validation must contain two components: first, a check on the representation of the atmospheric surface layer in the model and second, a check on the derived surface turbulent fluxes, that is, confirmation that the model bulk flux algorithms are well founded.

In this regard, Smith et al. (2001) compared the surface meteorological fields from the NCEP–NCAR reanalysis to high-quality ship observations made during the World Ocean Circulation Experiment (WOCE). They found that the reanalysis surface winds were underestimated at all latitudes, but there was better agreement with the surface air temperature and humidity fields. No direct turbulent heat flux measurements were used. Instead, the Smith (1988) bulk flux algorithm was employed to estimate the surface heat fluxes from the surface meteorological fields. Smith et al. (2001) found that the sensible and latent heat fluxes from the NCEP–NCAR reanalysis were too large when compared to estimates calculated from the surface fields.

In the Tropics, Bony et al. (1997) and Shinoda et al. (1999) compared NCEP–NCAR reanalysis fluxes with satellite and in situ observations and found overestimates in the latent heat flux of order 10 W m^{-2}. In the northeast Atlantic, Josey (2001) found overestimates in surface heat fluxes of the same order in both ECMWF and NCEP–NCAR reanalysis data as compared to buoy data.

Renfrew et al. (2002) investigated the ability of the ECMWF operational analysis and the NCEP–NCAR reanalysis to capture the variability in the surface meteorological and air–sea flux fields observed from the R/V *Knorr* during its 40-day cruise in the Labrador Sea region in the winter of 1997. During the cruise, surface layer meteorological variables and surface turbulent heat fluxes were directly measured. The direct turbulent heat flux observations are compared to several bulk flux algorithms in Bumke et al. (2002). They note that the algorithm of Smith (1988), with heat exchange coefficients updated to those of DeCosmo et al. (1996)—the so-called Smith/DeCosmo algorithm—compared well with the direct turbulence measurements. Renfrew et al. (2002) show that the NCEP–NCAR reanalysis was able to capture the synoptic variability of the surface meteorology in the region but that the heat fluxes had a systematic bias toward high values. They argue that this bias is the result of roughness length formulations for heat and moisture in the NCEP–NCAR reanalysis that are inappropriate in conditions of high winds. They show that this bias is greatest during events characterized by high winds and large air–sea temperature differences. An offline recalculation using the NCEP–NCAR surface layer meteorological data and the independently validated Smith/DeCosmo algorithm gives surface heat flux time series that agree much more closely with those observed.

Air–sea flux climatologies indicate that the western boundary currents of the North Atlantic and North Pacific Oceans are regions where there are large exchanges of sensible and latent heat flux between the ocean and atmosphere (e.g., Josey et al. 1999; Garnier et al. 2000; WGASF 2001). Observational studies have shown these fluxes to be largest during cold-air outbreaks, when a cold, dry air mass from the continent is advected over the relatively warm ocean (Agee and Howley 1977; Blanton et al. 1989; Grossman and Betts 1990; Xue et al. 1995). This is a similar situation to wintertime conditions over the Labrador Sea (e.g., Renfrew and Moore 1999). Hence, given the results discussed above, it seems reasonable to question the turbulent heat fluxes in the NCEP–NCAR reanalysis in the vicinity of the western boundary currents. In this paper, we investigate this hypothesis. In particular we compare the surface layer and surface turbulent heat flux fields from the NCEP–NCAR reanalysis to a variety of datasets that have been collected in the Gulf Stream and the Kuroshio regions. In section 2 the model and observational data are described. In section 3 a number of surface flux algorithms are reviewed. Then in section 4 there is a detailed comparison of observations and model data. Following this we present in section 5 ''adjusted'' fields of sensible and latent heat fluxes that we suggest are a more accurate representation of the air–sea exchange of heat and moisture over the western boundary currents. Conclusions are drawn in section 6.

2. Data

a. Model data

In this paper we make use of the results of the NCEP–NCAR reanalysis project (Kalnay et al. 1996). The idea behind this, and other reanalysis projects, is to generate a model-consistent dataset ideal for short-term climatological studies. To this end, the operational atmospheric model and analysis schemes were ''frozen'' and a comprehensive reanalysis of all available historical data was carried out. The model used in the NCEP–NCAR reanalysis was identical to the NCEP operational model that was active at the start of the reanalysis (11 January 1995), except at a lower resolution of T62 [about 210-km horizontal resolution; see Kalnay et al. (1996) for more details]. In the NCEP–NCAR project the period of reanalysis was 1948 to the present, although there are concerns regarding the quality of the reanalysis in the presatellite period (e.g., Kalnay et al. 1996; Hines et al. 2000). Here we will consider the 15-yr period from 1979 to 1993. This allows for an easy comparison with the results of the ECMWF 15-yr reanalysis (ERA-15) as well as other recent climatologies, such as the Southampton Ocean Centre climatology (Josey et al. 1998, 1999). In addition to the standard fields contained in any meteorological analysis, the NCEP–NCAR reanalysis includes fields, such as the surface turbulent heat fluxes, which are generated by the 6-h forecast cycle that is used to provide first-guess fields

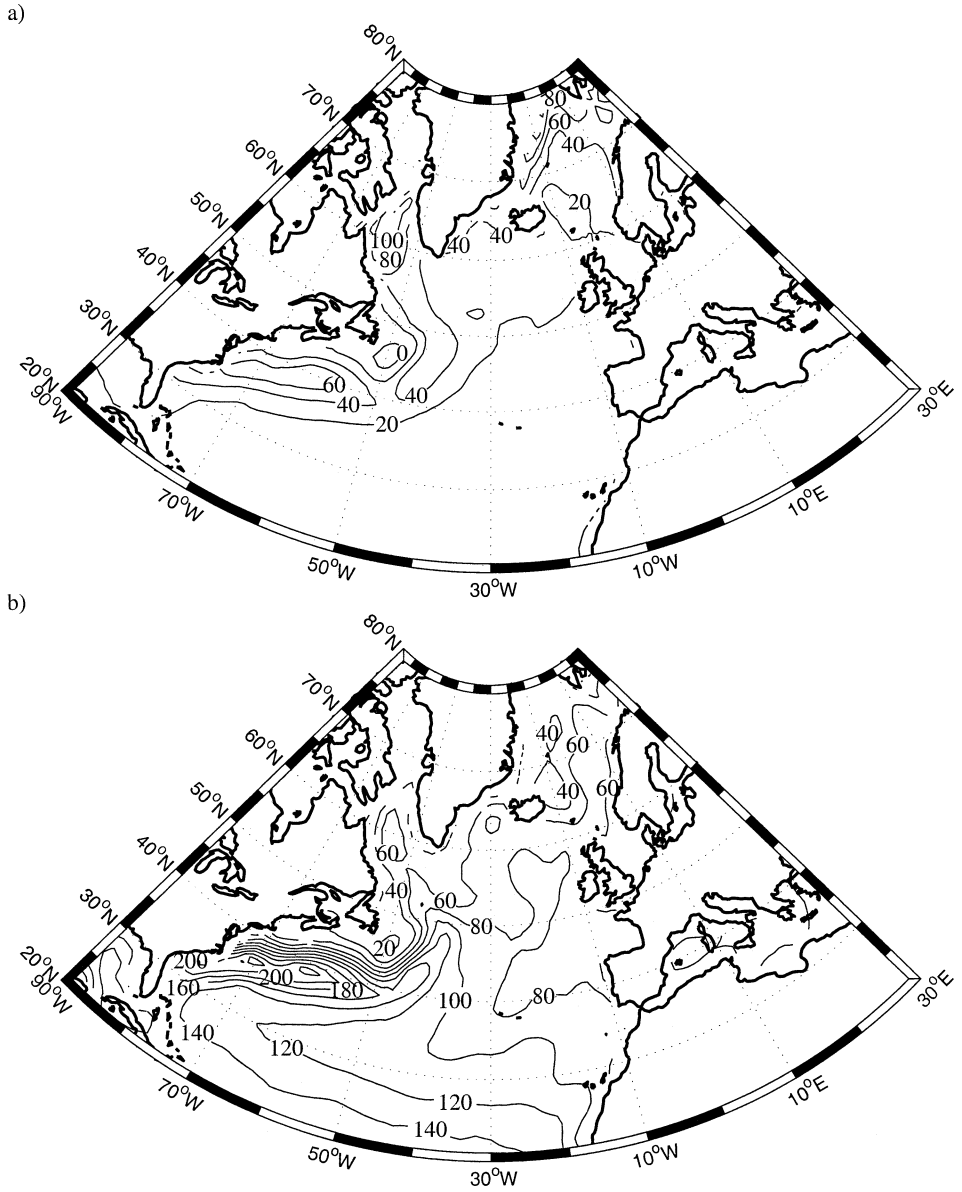

FIG. 1. Annual mean (a) sensible and (b) latent heat fluxes (W m^{-2}) from the NCEP–NCAR reanalysis over the North Atlantic Ocean. Climatology based on years 1979–93.

for the next data assimilation cycle. Produced in this way, the forecast-cycle fields are inherently more dependent on the model parameterizations than the analysis-cycle fields (Kalnay et al. 1996).

Figure 1 shows the annual mean sensible and latent heat flux fields from the NCEP–NCAR reanalysis over the North Atlantic Ocean for the period 1979–93. Note we use the convention that a positive flux represents a transfer of heat from the ocean to the atmosphere. From this figure, one can see the elevated sensible and latent heat fluxes that occur over the Gulf Stream. In addition, the Labrador and Norwegian Seas are regions where the sensible fluxes are large. In these regions, the colder surface air temperatures reduce the saturation vapor pressure thereby limiting the magnitude of the latent heat flux. Figure 2 shows the same fields for the North Pacific Ocean. The elevated sensible and latent heat fluxes over the Kuroshio (to the south and east of Japan) are evident. Large sensible heat fluxes also occur over the Sea of Japan, the Sea of Okhotsk, and the Bering Sea. The latent heat fluxes are generally larger than the sensible heat fluxes. Elevated latent fluxes also occur in the subtropical Pacific near the international dateline.

In Fig. 3, we present the annual cycle in monthly mean latent heat flux from the NCEP–NCAR reanalysis at locations centered in the regions of elevated heat fluxes in the Gulf Stream (37°N, 70°W) and Kuroshio (35°N, 144°E) regions. Also shown is the annual cycle

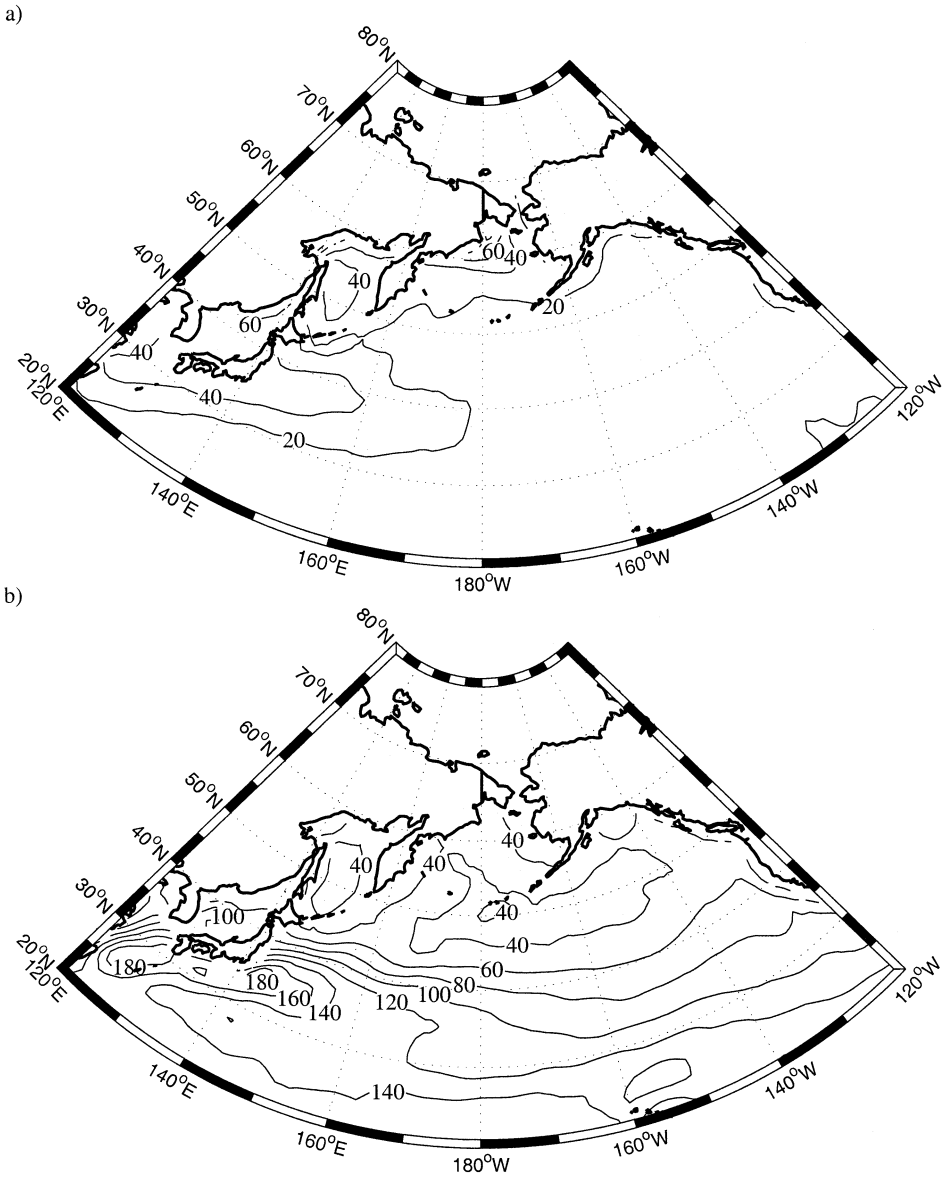

FIG. 2. As in Fig. 1 except for the North Pacific Ocean.

in the monthly mean standard deviation of the 6-hourly latent heat fluxes about the monthly mean values, that is, a measure of the variability in the magnitude of the latent heat flux during a particular month. The figure shows that in both regions there is a pronounced annual cycle in the magnitude of the latent heat flux. In both regions, the maximum, around 325 W m^{-2}, occurs in the winter months while the minimum, around 50–100 W m^{-2}, occurs in the summer months. The annual cycle is larger in magnitude over the Kuroshio than over the Gulf Stream. The standard deviation of the 6-hourly values about the monthly means also has a pronounced annual cycle, with maxima in the winter and minima in the summer. The standard deviations in the winter months are quite large, about 150–200 W m^{-2}, which implies considerable day-to-day variability in the magnitude of the flux about its monthly mean. We shall see that a representation of this variability is important if one is to generate accurate monthly mean values. Although not shown, qualitatively similar results hold for the annual cycle in the sensible heat flux in the two regions.

b. Observational data

From January to March 1986 a major field project, the Genesis of Atlantic Lows Experiment (GALE), was held off the eastern seaboard of the United States (Raman and Riordan 1988). The objective of the experiment was to improve the understanding of the genesis and

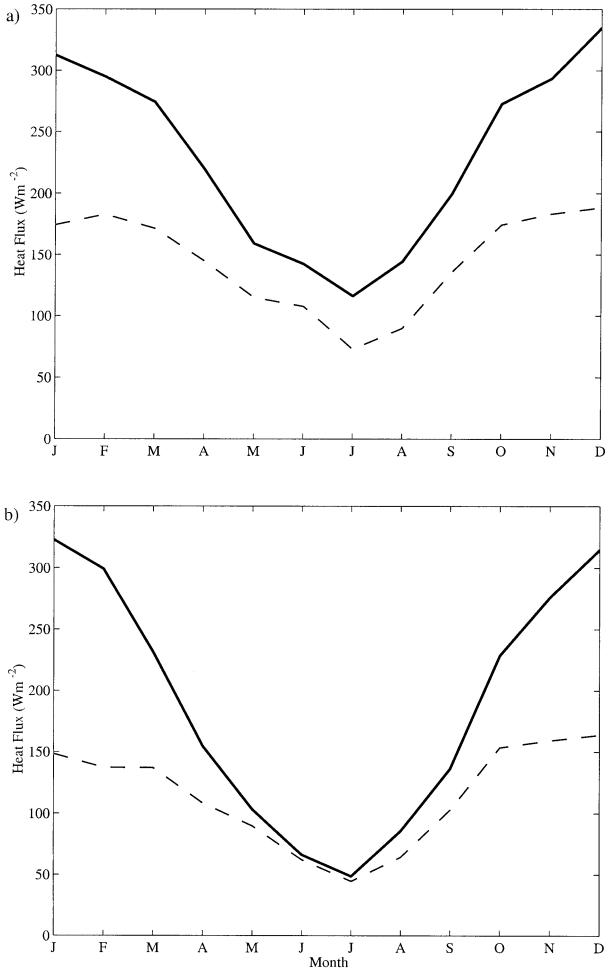

FIG. 3. Annual cycle of monthly mean latent heat flux (solid line) and monthly mean std dev of the 6-hourly latent heat flux (dashed line) at (a) 37°N, 70°W and (b) 35°N, 144°E.

development of winter storms in the region. A crucial component of the experiment was the documentation of air–sea interaction that takes place as cold and dry continental airflows over the warm surface waters of the Gulf Stream. To accomplish this, eight instrumented buoys were deployed offshore of North and South Carolina, and two research vessels were tasked with making measurements of surface and subsurface temperatures, salinities, and currents. In addition, the National Oceanic and Atmospheric Administration (NOAA) P-3 instrumented research aircraft collected 50 h of measurements on the structure of the atmospheric boundary layer and the magnitude of the air–sea fluxes in the region. For this study, we have chosen to use data collected during the second intensive observing period (IOP2) from 25–30 January 1986. Xue et al. (1995) synthesized all available data from IOP2 into space–time plots of the sensible and latent heat fluxes across a 250-km-long section of the Gulf Stream off South Carolina (shown in Fig. 4). The Xue et al. (1995) synthesis is unique in that it provides an estimate of the temporal variability of the fluxes over a period of several days in a region that approximates a grid box of the NCEP–NCAR reanalysis. It is therefore ideally suited to compare against the reanalysis fields.

The National Buoy Data Center of NOAA maintains a network of moored buoys in the coastal waters of the United States. Although the primary use of the buoys is in the preparation of marine forecasts, the data are archived and available for other purposes. The buoys routinely provide hourly measurements of the atmospheric pressure, temperature, and winds, as well as the sea surface temperature. Relative humidity measurements are not routinely made. Instruments are calibrated prior to deployment and are replaced with newly calibrated ones on a regular basis. There is evidence (Large et al. 1995) that the 10-m wind speed data from buoys are underestimated in high wind/wave conditions. No

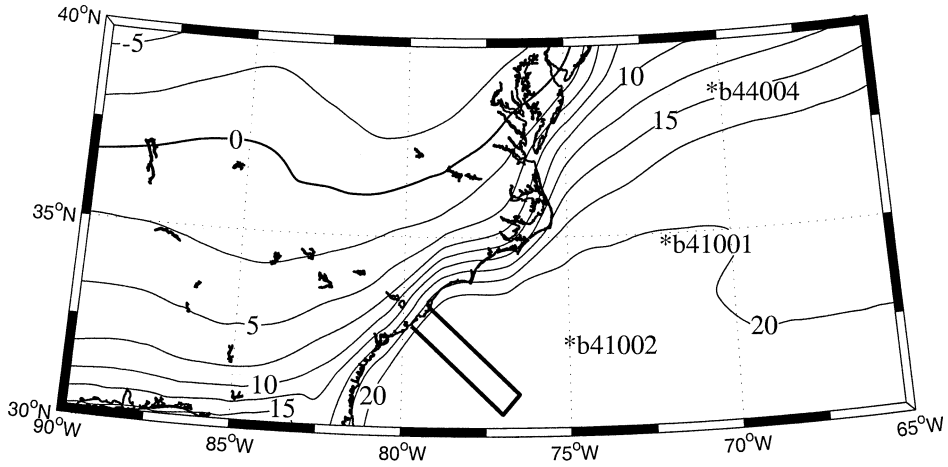

FIG. 4. Location of GALE IOP2 (box) and National Buoy Data Center (asterisks) data. The background field is the monthly mean surface temperature field (°C) for Jan from the NCEP–NCAR reanalysis.

attempt was made to account for this error. For comparison with the NCEP–NCAR fields, 6-hourly averages of the data were prepared. Here we make use of data from three buoys situated in the open ocean, off the eastern seaboard of the United States (identifiers 41001, 41002, and 44004), as shown in Fig. 4. From the buoy data, an estimate of the sensible heat flux was obtained using a bulk flux algorithm based on Smith (1988) with heat flux coefficients from DeCosmo et al. (1996), as discussed later.

Finally we also make use of observations from the University of Wisconsin–Milwaukee (UWM) Comprehensive Ocean–Atmosphere Data Set (COADS) climatology (da Silva et al. 1994). This is a global objective analysis of observed and derived surface marine parameters covering the period from 1945 to 1994. The climatology is based on individual observations, from research vessels and voluntary observing ships, found in the Comprehensive Ocean–Atmosphere Data Set (Slutz et al. 1985; Woodruff et al. 1987). Numerous bias corrections were made to the observations as discussed in da Silva et al. (1994). Estimates of the sensible and latent heat fluxes are derived from the marine observations using the bulk formulation of Large and Pond (1981, 1982). The data are available as monthly mean values on a $1^\circ \times 1^\circ$ grid.

Before proceeding with the comparison results, we briefly review how surface turbulent fluxes are calculated in bulk algorithms.

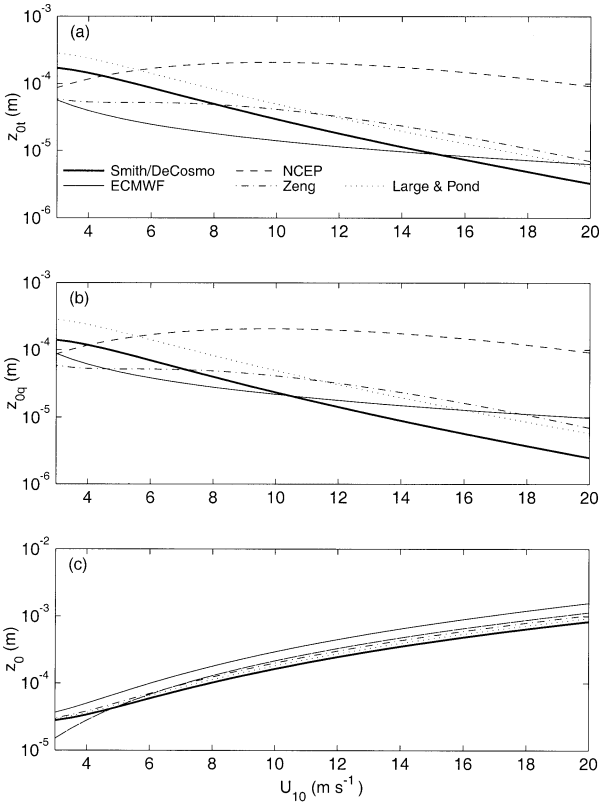

FIG. 5. Roughness lengths for heat, moisture, and momentum (z_{0t}, z_{0q}, and z_0) for various bulk flux algorithms, as a function of 10-m wind speed, for typical winter conditions over the Gulf Stream (see text).

3. Surface flux algorithms

Surface turbulent fluxes are calculated in numerical weather prediction models through bulk flux algorithms that relate standard meteorological variables to turbulent fluxes. In particular, the near-surface air temperature, wind speed, relative humidity, and sea surface temperature are used to calculate the surface sensible heat, latent heat, and momentum fluxes over water. The bulk flux algorithms are based on similarity theory and empirically tuned exchange coefficients, or equivalently, roughness lengths (Garratt 1992). In addition, the algorithms incorporate an adjustment for the stability of the atmospheric surface layer through stability-dependent ''ψ functions.'' The form of the ψ functions is well established; most models follow the standard Businger–Dyer relations (e.g., Paulson 1970; Businger et al. 1971; Dyer 1974), with some models implementing extensions for extremely stable or unstable conditions (e.g., Holtslag et al. 1990; Kader and Yaglom 1990; Grachev et al. 1998; Zeng et al. 1998). Such a consensus is not the case for the heat exchange coefficients, or the scalar roughness lengths, which are commonly used. Here a wide variety of functional forms are used for the same input data. The range is greatest for very high, or very low, wind speeds and for large air–sea temperature differences (Zeng et al. 1998; Renfrew et al. 2002). Renfrew et al. (2002) investigated wintertime air–sea fluxes over the Labrador Sea, a region subject to cold-air outbreaks over relatively warm waters (i.e., conditions where the bulk flux algorithms diverge in their calculated fluxes). They showed that the sensible and latent heat fluxes from the NCEP–NCAR reanalysis have a systematic bias toward high values in conditions of high heat flux, and that this was a result of an inappropriate roughness length formulation. The physics of high heat flux events over the western boundary currents are similar to those found in the Labrador Sea, and so it is reasonable to now question the NCEP–NCAR bulk algorithm for these regions.

To illustrate the range of roughness length functional forms in use, we present in Fig. 5 the roughness lengths for heat, moisture, and momentum for various bulk flux algorithms as a function of wind speed for typical conditions over the western boundary currents during the winter. In this case, there is a 2-m air temperature of 16°C, sea surface temperature (SST) of 20°C, and a relative humidity (RH) of 80%. These conditions are based on buoy data to be discussed below. The algorithms compared are two from leading modeling centers: those used in the NCEP–NCAR reanalysis and in the ECMWF operational model (also used in ERA-15); and three well-established empirically based algorithms:

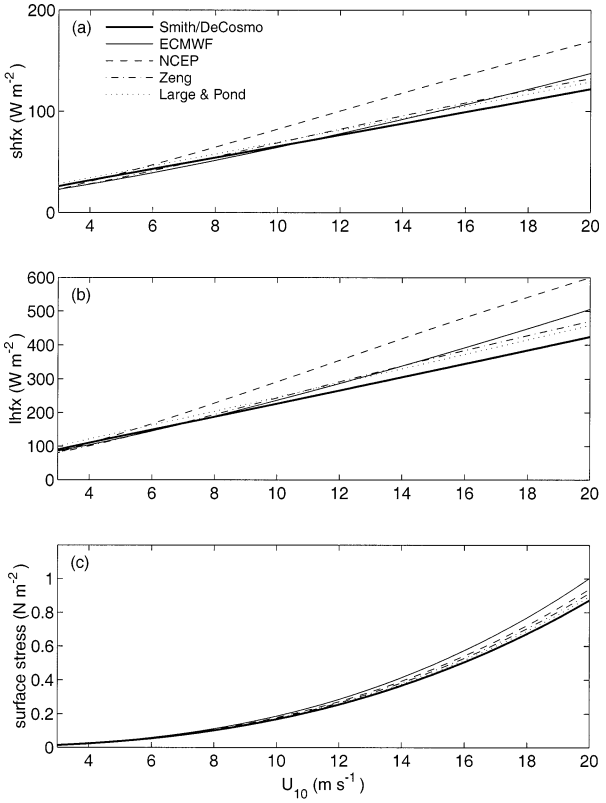

FIG. 6. Surface sensible heat flux, surface latent heat flux, and surface momentum flux for various bulk flux algorithms, as a function of 10-m wind speed, for typical winter conditions over the Gulf Stream (see text).

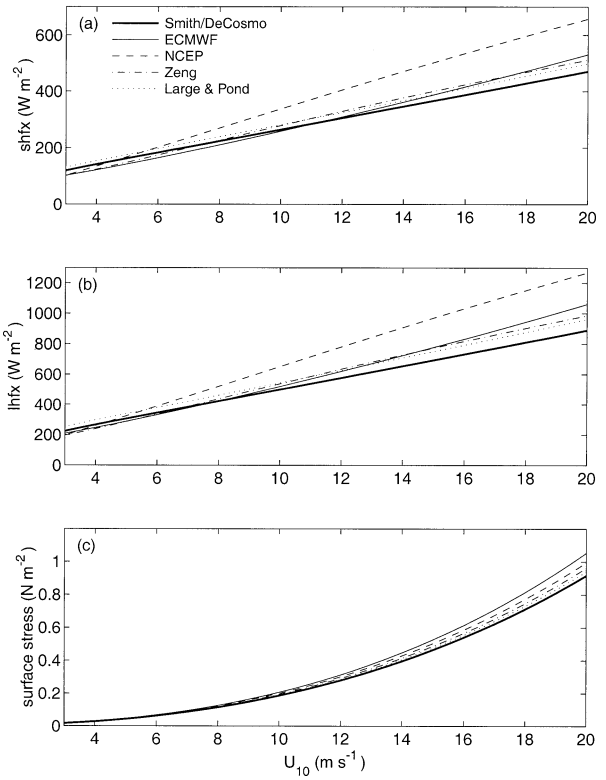

FIG. 7. As in Fig. 6, except for extreme conditions over the Gulf Stream (see text).

those of Smith/DeCosmo, Zeng et al. (1998), and Large and Pond (1981, 1982). The Smith/DeCosmo algorithm is based on Smith (1988), with heat flux coefficients updated after the Humidity Exchange over the Sea (HEXOS) experiment from DeCosmo et al. (1996). Recall heat fluxes from this algorithm compared well with in situ turbulent flux measurements during high heat flux conditions over the Labrador Sea (Bumke et al. 2002; Renfrew et al. 2002). Note also that the Southampton Oceanography Centre (SOC) air–sea flux climatology (Josey et al. 1998) is based on the algorithm of Smith (1988). The algorithm of Zeng et al. (1998) is based on a simplified version of the Tropical Ocean and Global Atmosphere Coupled Ocean–Atmosphere Response Experiment (TOGA COARE) 2.5 algorithm (Fairall et al. 1996), and was adopted for operational use by NCEP as of 15 June 1998 (H. L. Pan 2000, personal communication). The algorithm of Large and Pond (1981, 1982) is used in the UWM/COADS air–sea flux climatology of da Silva et al. (1994).

Figure 5 clearly shows that the roughness lengths for heat and moisture from the NCEP–NCAR reanalysis are outliers with respect to those from the other four algorithms. This is especially true at moderate to strong wind speeds. In contrast, the roughness lengths for momentum among the various algorithms are relatively similar, the small differences are due to small differences in the value of the Charnock constant used in the formulation (Zeng et al. 1998; Renfrew et al. 2002). As discussed by Renfrew et al. (2002), this implies that given the same environmental conditions and stability corrections, the NCEP surface layer parameterization should generate greater fluxes of sensible and latent heat than those of the other algorithms.

To illustrate this point, we present in Figs. 6 and 7 sensible heat, latent heat, and momentum fluxes for the same five bulk flux algorithms as a function of wind speed. Figure 6 is an illustration for the same, typical conditions used to generate Fig. 5, while Fig. 7 is for extreme conditions over the western boundary currents during winter based on the cold-air outbreak observations of Grossman and Betts (1990) and Xue et al. (1995). In this case there is a 2-m air temperature of 5°C, a SST of 20°C, and an RH of 60%. For the sake of this illustration, the fluxes are calculated with identical stability adjustments (standard Businger–Dyer ψ functions), thus isolating the effects of the different roughness length formulations used in the algorithms (Renfrew et al. 2002). As suggested by Fig. 5, Figs. 6 and 7 clearly show that for these input data, the bulk flux algorithm used in the NCEP–NCAR reanalysis is an outlier with respect to the other algorithms. The magnitude of the bias present in the NCEP–NCAR for-

TABLE 1. A comparison of sensible and latent heat fluxes for typical conditions (2-m air temperature of 16°C, SST of 20°C, RH of 80%, and 10-m wind speed of 10 m s^{-1}) and extreme conditions (2-m air temperature of 5°C, SST of 20°C, RH of 60%, and 10-m wind speed of 20 m s^{-1}) for various bulk flux algorithms. The final row shows a mean of the previous four values (excluding the NCEP–NCAR algorithm) ±15%.

	Typical conditions		Extreme conditions	
Bulk flux algorithm	Sensible heat flux (W m^{-2})	Latent heat flux (W m^{-2})	Sensible heat flux (W m^{-2})	Latent heat flux (W m^{-2})
NCEP–NCAR	82	292	657	1267
Smith/DeCosmo	65	227	470	889
Zeng et al. (1998)	69	244	511	986
ECMWF	64	236	531	1060
Large and Pond (1981, 1982)	69	246	498	961
Mean ± 15%	67 ± 10	238 ± 36	503 ± 75	974 ± 146

mulation increases with increasing wind speed. It is also greater for higher air–sea temperature differences and lower relative humidities during the extreme conditions.

Table 1 summarizes the behavior of the bulk flux algorithms at 10 and 20 m s^{-1}. There is an inherent uncertainty in relating surface layer data to surface fluxes using bulk algorithms, as a result of the approximations in the boundary layer physics that must be made. In a discussion of this Garratt (1992) suggests an uncertainty of order ±15% in the air–sea turbulent heat exchange. In the final row of Table 1, mean fluxes ±15% are noted, where the mean values are from the preceding four algorithms, excluding the NCEP–NCAR algorithm as an obvious outlier. In each case, all the bulk algorithm flux values are within the uncertainty limits, with respect to one another, while the NCEP–NCAR algorithm is outside the uncertainty limits.

4. Results

a. A comparison with GALE IOP2 observation

The second intensive observing period of GALE took place from 25 to 30 January 1986. At the beginning of the period, a low pressure system was located to the west of Lake Superior; associated with this system was an intense cold front leading a cold and dry air mass. By the 28th, the system had deepened and moved eastward, so that its center was over the Gulf of Saint Lawrence. As a consequence of its movement and intensification, strong northwesterly flow was established over much of the eastern United States, which resulted in the advection of cold and dry air over the eastern seaboard and Gulf Stream region. On the 28th, the Challenger Space Shuttle explosion occurred during takeoff from Florida. A contributing factor in this explosion was the extremely cold temperatures in Florida in the hours preceding the launch (Rogers 1986). Over the Gulf Stream, the combination of a large air–sea temperature contrast and high winds resulted in large fluxes of sensible and latent heat from the ocean to the atmosphere. Direct turbulence measurements from aircraft (Grossman and Betts 1990) and bulk estimates from buoy data (Xue et al. 1995) suggest that the total turbulent heat flux (sum of sensible and latent heat fluxes) was in excess of 1000 W m^{-2}. In Fig. 8, we present a *NOAA-9* Advanced Very High Resolution Radiometer (AVHRR) infrared satellite image from 0745 UTC on the 28th. The frontal clouds associated with the low pressure system can be seen along 70°W, as well as the low-level convective streamer clouds over the Gulf Stream and Gulf of Mexico. These linear and cellular clouds are a manifestation of the large fluxes of heat and moisture from the ocean into the atmosphere that were occuring.

Xue et al. (1995) synthesized all available GALE data for this period to show the temporal evolution of the sensible and latent heat fluxes over a region of the Gulf Stream off South Carolina (Fig. 4). In Fig. 9, we present these data as well as time series extracted from the nearest grid point of the NCEP–NCAR reanalysis, and a

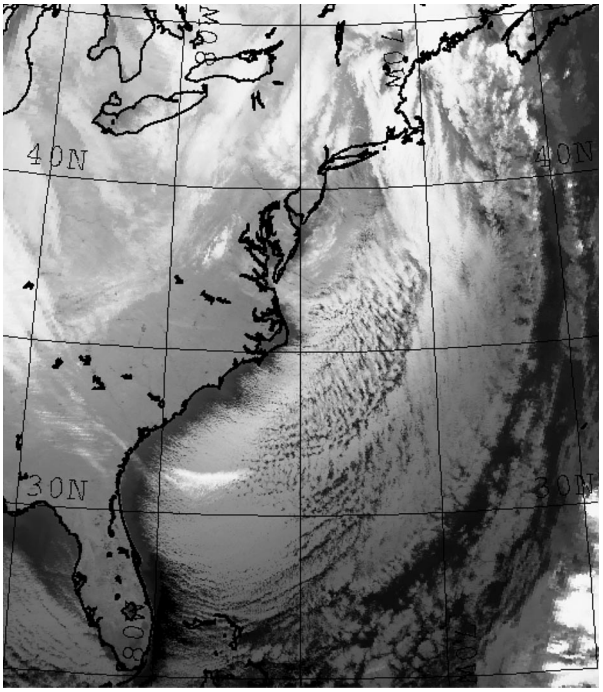

FIG. 8. *NOAA-9* AVHRR infrared image of the eastern seaboard of the United States from 0745 UTC 28 Jan 1986.

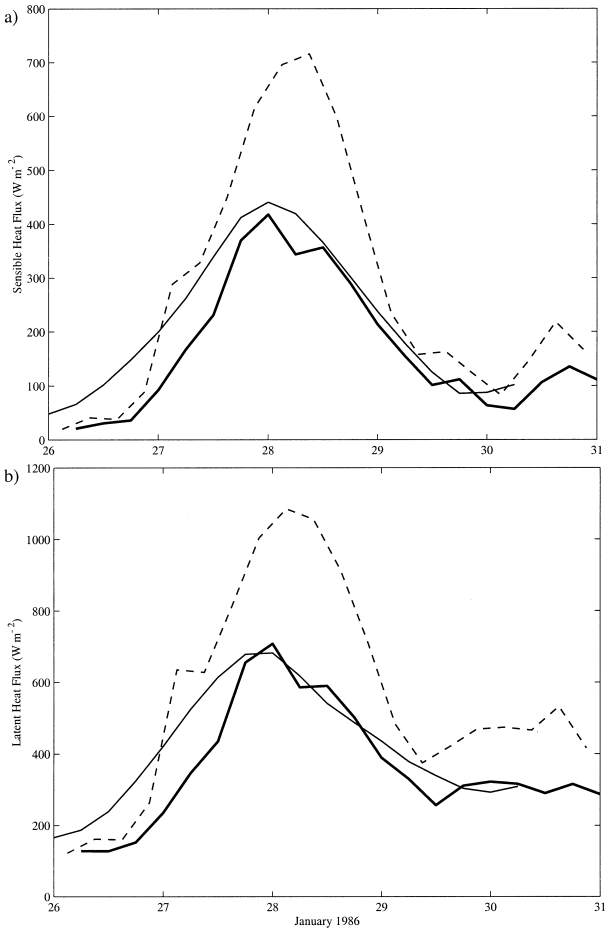

FIG. 9. Evolution of the (a) sensible and (b) latent heat flux (W m^{-2}) over the Gulf Stream off Cape Hatteras 26–30 Jan 1986. The thin solid lines represent the estimates from Xue et al (1995). The dashed lines represent the fluxes from the NCEP–NCAR reanalysis. The thick solid lines represent the NCEP-adjusted fluxes. Positive values indicate a flux out of the ocean.

''recalculated'' flux estimate using the near-surface meteorological fields of the NCEP–NCAR reanalysis and the Smith/DeCosmo bulk flux algorithm discussed earlier. From now on we shall refer to such recalculated NCEP–NCAR fluxes as ''NCEP-adjusted'' fluxes. From Fig. 9 it is clear that there was a rapid increase in the magnitude of the fluxes between 26 and 28 January. Xue et al. (1995) estimate that the peak sensible and latent heat fluxes (of about 400 and 600 W m^{-2}, respectively) occurred around 0000 UTC on the 28th and were followed by a rapid decrease in the magnitude of the fluxes. The magnitude of the peak fluxes is consistent with direct turbulent measurements made from aircraft on the 28th (Grossman and Betts 1990).

Comparing the three time series, the NCEP–NCAR reanalysis data represent significant overestimations of both the sensible and latent heat fluxes. According to the reanalysis, the peak sensible and latent heat fluxes on the 28th were about 700 and 1000 W m^{-2}, respectively, which corresponds to an approximate 70% overestimation in the magnitude of the total turbulent heat flux. In addition, the rapid increase in surface fluxes occurs about 12 h later in the NCEP model than is observed. The NCEP-adjusted heat fluxes are in excellent agreement with the observations of Xue et al. (1995) with respect to magnitude, and are in good agreement with respect to phasing. The difference between the NCEP–NCAR reanalysis fluxes and the NCEP-adjusted fluxes is of similar size to the differences illustrated in the extreme western boundary current conditions of Fig. 7 and Table 1. Note that one would not expect the differences to be exactly explained by these illustrations, recalling the NCEP-adjusted fluxes are from an offline calculation. They are not equivalent to implementing the Smith/DeCosmo algorithm into the NCEP model, because in this scenario interactions with the development of the model's boundary layer would lead to both different surface heat fluxes and different surface layer meteorological fields. Notwithstanding this point, the NCEP-adjusted flux results provide convincing, indirect evidence that the reanalysis surface layer is adequately represented in this case, and it is the bulk flux algorithm that is in question.

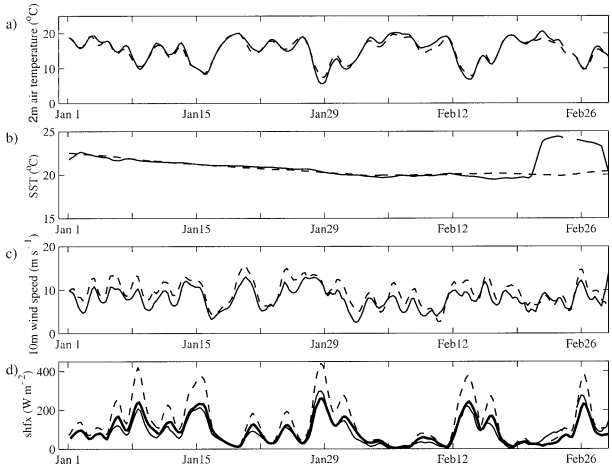

FIG. 10. Time series of (a) 2-m air temperature (°C), (b) sea surface temperature (°C), (c) 10-m wind speed (m s^{-1}), and (d) sensible heat flux (W m^{-2}) at buoy 41001 during Jan and Feb 1986. The thin solid lines represent these fields as observed from the buoy. The dashed lines represent these fields as extracted from the NCEP–NCAR reanalyses. In (d), the buoy sensible heat fluxes are calculated using the Smith/DeCosmo bulk flux algorithm, and the thick solid line represents the NCEP-adjusted sensible heat flux.

b. A comparison with Gulf Stream buoy data

To begin our comparison with the buoy data, we continue with a discussion of the GALE period. Figure 10 compares observations from buoy 41001 during January and February 1986 and time series extracted from the NCEP–NCAR reanalysis. Note that buoy 41002, which is closer to the GALE IOP2 area, was not operational

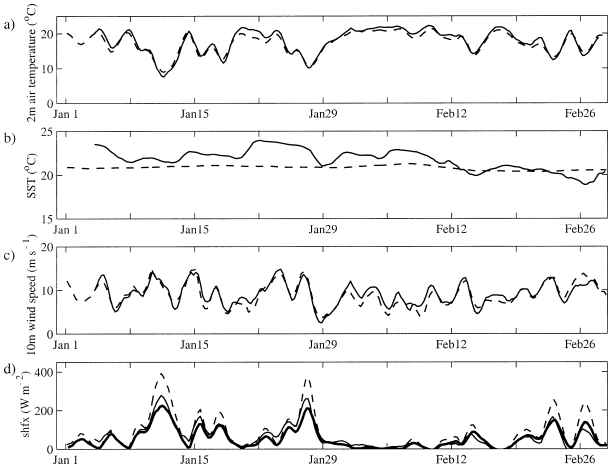

FIG. 11. As in Fig. 10, except for buoy 41002 during Jan and Feb of 1982.

during this period. The panels show the 2-m air temperature, the SST, the 10-m wind speed, and the sensible heat flux. The buoy sensible heat fluxes are calculated using the Smith/DeCosmo algorithm. Also included are NCEP-adjusted sensible heat fluxes (calculated as above).

Intrusions of cold air over the buoy location are seen to be a common occurrence during this period. In general, the NCEP–NCAR reanalysis is able to capture these intrusions, although there is a tendency to underestimate the coldest air temperatures. For the most part the SST is also well represented in the NCEP–NCAR reanalysis, although the large SST increase that occurred near the end of February was not captured. It is unclear what caused this, but one possibility is the presence of a Gulf Stream ring (Olson 1991) that was too small to be captured in the SST analysis used in the NCEP–NCAR reanalysis (Reynolds and Smith 1994). For this period, the NCEP–NCAR reanalysis is able to capture the variability in the 10-m wind speeds, although there appears to be a slight overestimation at times. In marked contrast, the sensible heat flux in the NCEP–NCAR reanalysis represents a large overestimate, especially in situations of high winds and large air–sea temperature contrasts. For example on 28 January 1986, the GALE IOP2 event, the sensible heat flux from the NCEP–NCAR reanalysis exceeded the buoy estimate by approximately 125 W m^{-2} (about 50%). There is much better agreement between the calculated buoy sensible fluxes and the NCEP-adjusted fluxes. There is a small systematic underestimation in the recalculated fluxes due to a smaller NCEP air–sea temperature difference than that observed, although note this is partially compensated for by an overestimation in the 10-m wind speeds. It should be noted that during the GALE IOP2 event, the sensible heat fluxes at the buoy position are lower than those of Fig. 9. This can be explained by the lower SSTs reducing the air–sea temperature difference compared to those farther south (Fig. 4).

TABLE 2. A comparison of observed and NCEP–NCAR reanalysis mean surface meteorological and sensible heat fields during Jan at operational buoy locations along the eastern seaboard of North America.

Buoy	10-m wind speed (m s^{-1})	2-m air temperature (°C)	SST (°C)	Sensible heat flux (W m^{-2})	
41001	9.6	15.0	20.7	89	Observations
	9.7	15.8	20.4	120	NCEP–NCAR
				81	NCEP-adjusted
41002	8.6	17.6	22.1	70	Observations
	8.0	17.6	22.0	101	NCEP–NCAR
				68	NCEP-adjusted
44004	9.0	8.3	14.6	109	Observations
	9.9	9.6	14.3	125	NCEP–NCAR
				83	NCEP-adjusted

Figure 11 shows a similar time series for buoy 41002 during January and February 1982. With regards to the 2-m air temperature, there is good agreement between the NCEP–NCAR reanalysis and the buoy data again. In contrast, there is considerable disagreement with respect to the SST time series. This buoy is located in a region where there is considerable lateral movement in the location of the Gulf Stream (Xue et al. 1995). The relatively coarse spatial and temporal resolution of the SST used in the reanalysis appears to be unable to resolve this variability. Comparing the 10-m wind speeds, there is again good agreement between the observations and the reanalysis. But for the sensible heat fluxes, again the reanalysis significantly overestimates the buoy derived flux estimates and the NCEP-adjusted estimates. This is especially true during conditions of high winds and large air–sea temperature contrasts.

We summarize our buoy data comparison with some mean statistics comparing the buoy observations and the reanalysis. In computing the mean values, we consider all Januarys during the period under investigation (1979–93) for which the coverage of buoy data was at least 90%. This results in 8 months of data for buoys 41001 and 41002, and 11 months of data for buoy 44004. Table 2 presents a comparison of the surface layer and sensible heat flux data at the three buoy locations with corresponding values from the NCEP–NCAR reanalysis. As above, the sensible heat fluxes derived from the buoy observations were calculated with the Smith/DeCosmo bulk algorithm. Overall the NCEP–NCAR surface fields are in good agreement with the observations. The largest discrepancies exist for the temperature fields at buoy 44004, which is located north of Cape Hatteras on the shoreward flank of the Gulf Stream in a region characterized by large gradients in sea surface temperatures (Fig. 4). We attribute the discrepancies at this location to an inability of the NCEP–NCAR reanalysis to resolve these SST gradients. Taking all three buoys into consideration, there does not seem

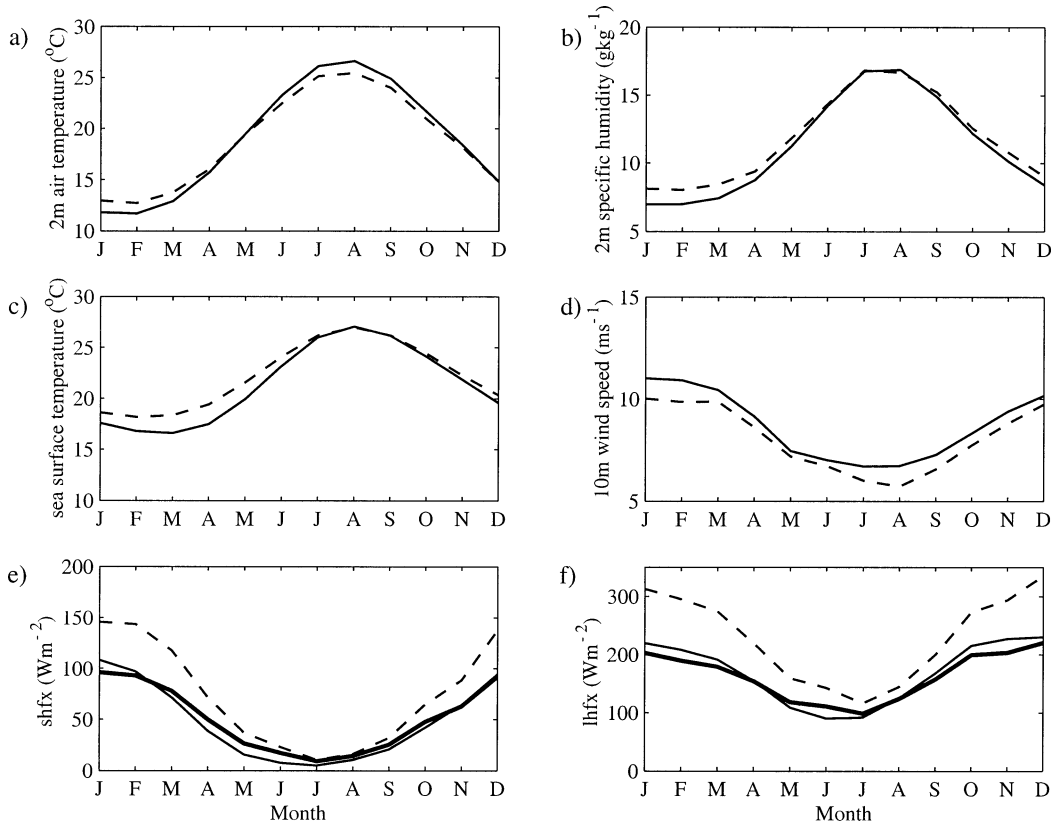

FIG. 12. Annual cycle of (a) the 2-m air temperature (°C), (b) the 2-m specific humidity (g kg^{-1}), (c) the sea surface temperature (°C), (d) the 10-m wind speed (m s^{-1}), (e) the sensible heat flux (W m^{-2}), and (f) the latent heat flux (W m^{-2}) at a location in the Gulf Stream region (37°N, 70°W). The thin solid lines represent these fields as extracted from the UWM/COADS climatology. The dashed lines represent these fields as extracted directly from the NCEP–NCAR reanalysis. The thick solid lines in (e) and (f) represent NCEP-adjusted sensible and latent heat fluxes.

to be any systematic biases in wind, air temperature, or sea surface temperature. In agreement with the results found for the two cases described above, the sensible heat flux from the NCEP–NCAR reanalysis is significantly larger than that deduced directly from the observations. This is true despite the good agreement found between the surface layer meteorological observations and the reanalysis values. The NCEP-adjusted sensible heat fluxes are in much better agreement with those derived from the buoy observations, except at buoy 44004, where the NCEP–NCAR reanalysis is unable to adequately resolve the observed SST gradients.

c. A comparison with UWM/COADS data

We conclude this section with a comparison of the NCEP–NCAR reanalysis surface layer and turbulent heat flux fields with those from the UWM/COADS dataset. In Figs. 12 and 13, we present the annual cycle, in terms of monthly means, of the 2-m air temperature, the 2-m specific humidity, the SST, the 10-m wind speed, the sensible heat flux and latent heat flux from the UWM/COADS dataset, and the NCEP–NCAR reanalysis. Figure 12 is for a location centered in the region of intense air–sea interaction in the Gulf Stream (37°N, 70°W); Fig. 13 is for a similar location in the Kuroshio (35°N, 144°E). Included in the bottom two panels are NCEP-adjusted estimates of the surface heat fluxes (derived as above). Overall it is evident that the annual cycles in the surface layer fields from the NCEP–NCAR reanalysis agree well with those from UWM/COADS. There appear to be some small systematic differences—an underestimate of wind speed and an overestimate in humidity at both locations throughout the year. Similar such problems were noted in Weller et al. (1998), Renfrew et al. (2002), and Smith et al. (2001). The agreement in the Kuroshio region tends to be somewhat poorer than in the Gulf Stream region.

Comparing the turbulent heat fluxes, the monthly mean NCEP–NCAR values are significantly larger than those from UWM/COADS. The differences are greatest during the winter months. Tables 3 and 4 summarize the comparison. The sensible and latent flux rms errors are 62% and 40% (for the Gulf Stream) and 41% and 27% (for the Kuroshio), considerably higher than one would expect from the relatively small differences in the surface layer fields. Indeed comparing the NCEP-adjusted fluxes to the observation, the rms errors are on

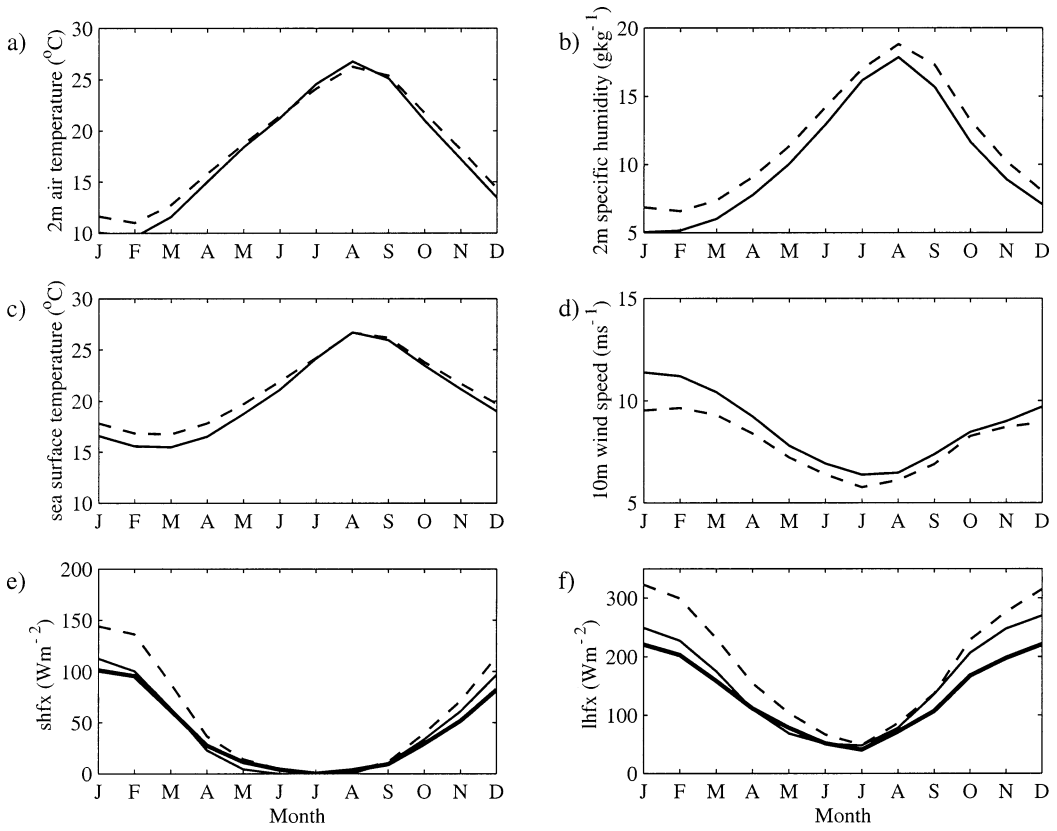

FIG. 13. As in Fig. 12, except for a location over the Kuroshio (35°N, 144°E).

the order of 15%, a similar size to that which would be expected given the approximate 10% rms errors in the meteorological data.

In summary, all three comparisons in this section show a systematic bias in the sensible and latent heat flux fields from the NCEP–NCAR reanalysis. This bias results in overestimates in the magnitudes of the surface heat fluxes in both the Gulf Stream and Kuroshio. These are most pronounced during high heat flux events that, in these regions, are characterized by high wind speeds and large air–sea temperature contrasts. Our comparison of the surface layer fields in these regions did not identify any systematic biases that could explain these results. Instead, as discussed by Zeng et al. (1998) and Renfrew et al. (2002), this systematic bias is the result of roughness length formulations for heat and moisture in the NCEP–NCAR reanalysis, which are inappropriate in conditions of high winds. The bias increases with increasing air–sea temperature differences. A much better agreement with observations is obtained when the surface layer fields from the reanalysis were used offline, with a bulk algorithm following Smith (1988) and DeCosmo et al. (1996), to generate new estimates of the sensible and latent heat fluxes. These are referred to here as the NCEP-adjusted fluxes.

5. Surface heat flux fields calculated from adjusted NCEP surface layer data

Following the results of the previous two sections, we have recalculated offline global fields of surface sensible and latent heat fluxes using the NCEP–NCAR re-

TABLE 3. Comparison of winter mean values for surface layer fields from UWM/COADS and the NCEP–NCAR reanalysis at a location over the Gulf Stream (37°N, 70°W). Rms errors are with respect to UWM/COADS.

	10-m wind speed ($m\ s^{-1}$)	2-m air temperature (°C)	2-m specific humidity ($g\ kg^{-1}$)	SST (°C)	Sensible heat flux ($W\ m^{-2}$)	Latent heat flux ($W\ m^{-2}$)
UWM/COADS	8.7	18.9	11.2	21.4	48	170
NCEP–NCAR	8.0	18.8	11.8	22.2	74	230
Rms error	4%	6%	5%	8%	62%	40%
NCEP-adjusted					51	163
Rms error					15%	7%

TABLE 4. Comparison of winter mean values for surface layer fields from UWM/COADS and the NCEP–NCAR reanalysis at a location over the Kuroshio (35°N, 144°E). Rms errors are with respect to UWM/COADS.

	10-m wind speed ($m\ s^{-1}$)	2-m air temperature (°C)	2-m specific humidity ($g\ kg^{-1}$)	SST (°C)	Sensible heat flux ($W\ m^{-2}$)	Latent heat flux ($W\ m^{-2}$)
UWM/COADS	8.6	17.8	10.4	20.4	42	155
NCEP–NCAR	7.9	18.5	11.6	21.0	55	189
Rms error	5%	13%	4%	10%	41%	27%
NCEP-adjusted					40	135
Rms error					16%	18%

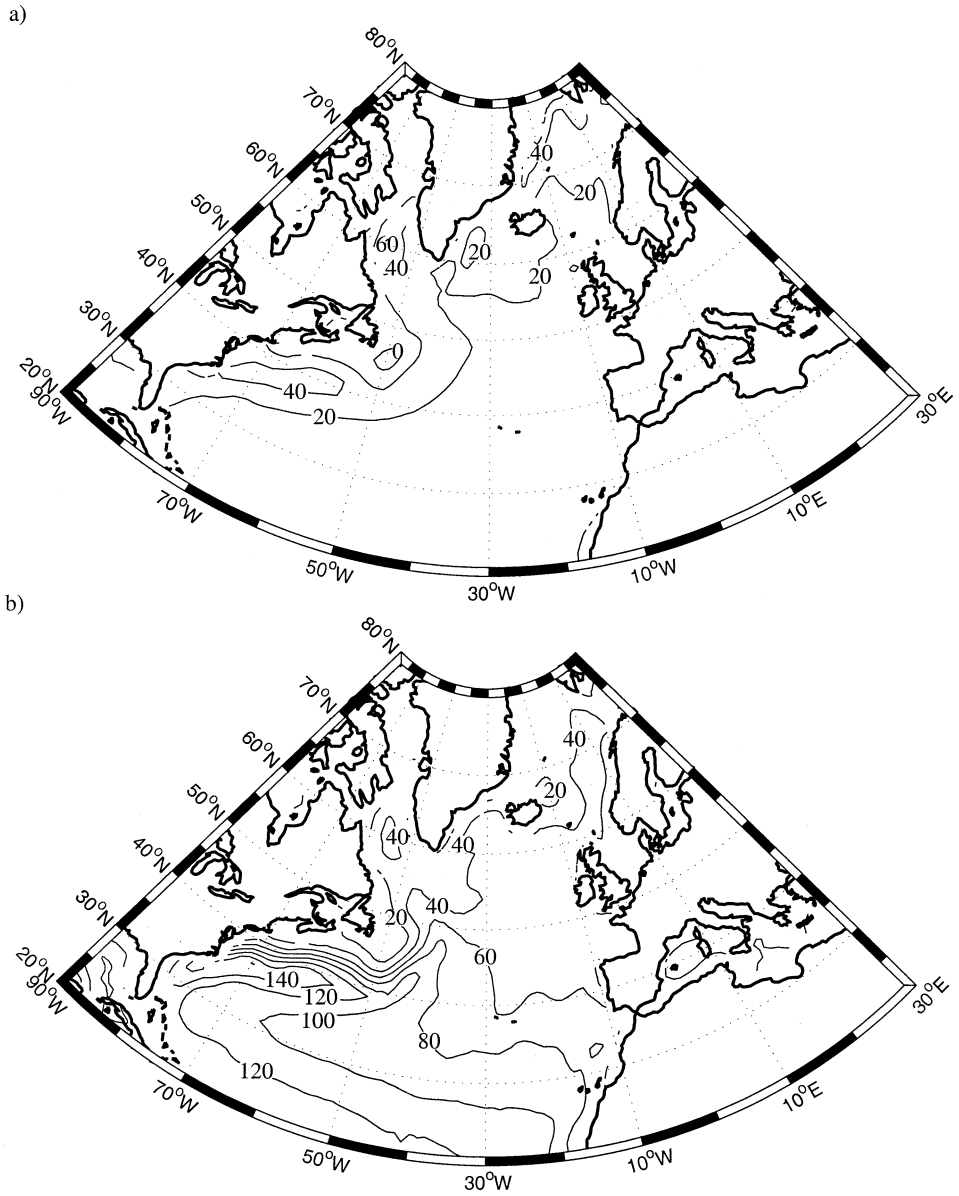

FIG. 14. Annual mean NCEP-adjusted (a) sensible and (b) latent heat fluxes ($W\ m^{-2}$) over the North Atlantic Ocean. Climatology based on years 1979–93.

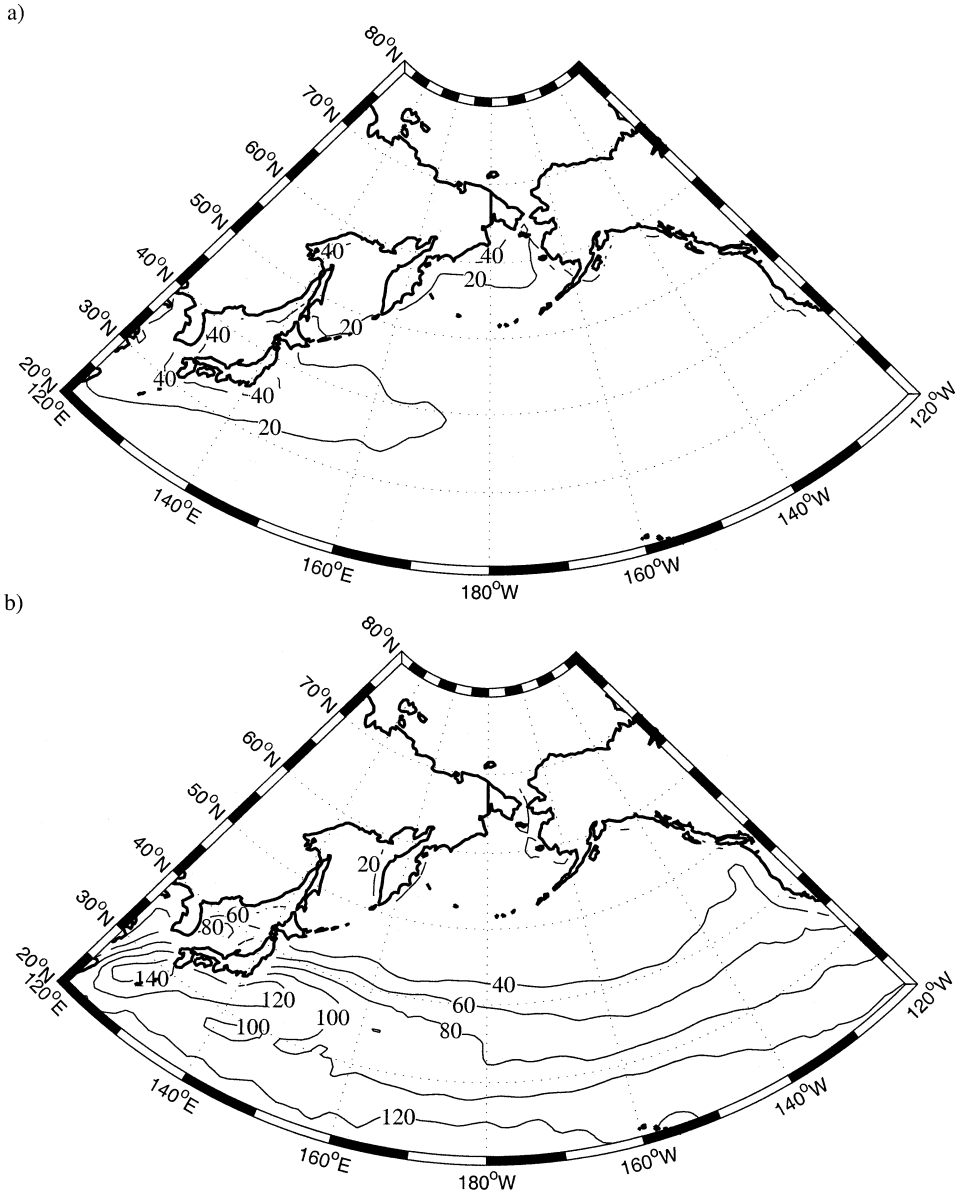

FIG. 15. As in Fig. 14, except for the North Pacific Ocean.

analysis surface layer meteorological fields and the Smith/DeCosmo bulk algorithm, that is, global NCEP-adjusted fields. Figure 14 shows the annual mean sensible and latent flux fields over the North Atlantic Ocean based on the years 1979–93. The heat fluxes were calculated every 6 h and averaged to produce the fields presented. Figure 15 presents the same fields for the North Pacific Ocean. Comparing Figs. 14 and 15 with Figs. 1 and 2, one can see that there is a significant reduction in the magnitude of the fluxes over all of both ocean basins. The largest changes occur over the western boundary currents and the high latitude marginal seas. For example, the annual mean peak latent heat fluxes in the Gulf Stream are now about 160 W m^{-2} compared to over 230 W m^{-2}, and over the Kuroshio they are now about 150 W m^{-2} compared to 200 W m^{-2}. These changes, which are not restricted to the western boundary currents, are significant enough to have a global impact. The global oceanic mean sensible and latent heat fluxes (for 1979–93) from the NCEP–NCAR reanalysis are 13.2 and 96.6 W m^{-2}, and from the NCEP-adjusted data are 11.1 and 79.4 W m^{-2}.

Table 5 presents a comparison of the maximum annual mean turbulent heat fluxes over the Gulf Stream and Kuroshio for the NCEP–NCAR reanalysis, the NCEP-adjusted fluxes, and a number of other recent air–sea flux climatologies. When comparing the sensible heat fluxes, as we would expect from the results for the pre-

TABLE 5. Maximum annual mean sensible and latent heat flux over the Gulf Stream and Kuroshio regions from a variety of climatologies. All climatologies are based on the years 1979–93 except for the SOC, which is based on 1980–93. The final row shows a mean of the previous three values (excluding those based on NCEP–NCAR) ±15%.

	Gulf Stream		Kuroshio	
Dataset	Sensible heat flux (W m^{-2})	Latent heat flux (W m^{-2})	Sensible heat flux (W m^{-2})	Latent heat flux (W m^{-2})
NCEP–NCAR	75	230	77	200
NCEP-adjusted	51	166	52	152
ERA-15	58	211	51	184
UWM/COADS	57	185	68	169
SOC	42	188	38	181
Mean ± 15%	52 ± 8	194 ± 29	52 ± 8	178 ± 26

vious two sections, the NCEP–NCAR values are considerably larger than the other estimates. The NCEP-adjusted sensible heat fluxes are broadly similar to the in situ climatologies and to ERA-15. Certainly they are within the ±15% estimate of uncertainty placed upon the use of bulk flux algorithms to calculate surface turbulent fluxes (Garratt 1992). The lowest values are from the SOC climatology, which are likely to be due in part to their use of the Smith (1988) heat exchange coefficient, which is lower than the other coefficients used. Smith (1988) recommends a coefficient of 1.0×10^{-3} whereas DeCosmo et al. (1996) recommend 1.14×10^{-3}. Comparing the latent heat fluxes, both the NCEP–NCAR reanalysis and the ERA-15 reanalysis appear high compared to the in situ climatologies and the NCEP-adjusted values. Note that these values contain a multitude of small differences (e.g., in meteorological data, flux algorithms, sampling, and analysis procedures). At present it is extremely difficult to say which overall flux climatology is most accurate. Indeed, as concluded by the WGASF (2001), all flux climatologies have their advantages and their disadvantages, and all are far from perfect.

There is a pronounced annual cycle in the turbulent heat fluxes over the western boundary currents with the largest monthly mean fluxes occurring during the winter months (e.g., Figs. 3, 12, 13). Furthermore, the instantaneous fluxes during the winter months can be significantly larger than the monthly mean values (Fig. 3). It is during these high heat flux events that the bias in the NCEP–NCAR heat fluxes is largest, and it therefore follows that the reductions in the magnitude of the air–sea fluxes should be more pronounced during the winter months. This is confirmed in Fig. 16 where the difference between the NCEP–NCAR reanalysis and the NCEP-adjusted latent heat flux over the North Atlantic is displayed for winter [December–January–February (DJF)] and summer [June–July–August (JJA)]. During the winter months, there is a 100 W m^{-2} reduction in the magnitude of the latent heat flux over the Gulf Stream. In contrast, there is only a 20 W m^{-2} reduction during the summer months. Similar reductions also occur for the sensible heat flux, especially over the high latitude marginal seas.

6. Conclusions

Over the western boundary currents of the North Atlantic and North Pacific Oceans, the surface sensible and latent heat fluxes from the NCEP–NCAR reanalysis are overestimated. This overestimate is largest in magnitude in the winter months during high heat flux events, characterized by high wind speeds and large air–sea temperature differences. In contrast, the surface layer meteorological fields are adequately represented in the NCEP–NCAR reanalysis.

In both typical and extreme atmospheric conditions over the western boundary currents, the surface layer parameterization used in the NCEP–NCAR reanalysis is an outlier with respect to a variety of other parameterizations, including three well-established algorithms that have been constrained to agree with a number of observational datasets. It is suggested that the use of this inappropriate roughness length formulation in the reanalysis is the cause of the overestimate in the turbulent heat fluxes. These conclusions are consistent with those reached by Renfrew et al. (2002) for the Labrador Sea, a typical high latitude marginal sea. Hence, we would suggest that care must be taken in using the NCEP–NCAR reanalysis turbulent heat fluxes in driving ocean models, or in budget studies, where the domain includes the western boundary currents or high latitude marginal seas.

We have made use of the reasonable quality of the surface layer meteorological fields from the NCEP–NCAR reanalysis to present adjusted global surface turbulent heat flux fields. These fields were calculated offline with a well-established bulk flux algorithm, based on Smith (1988) with coefficients from DeCosmo et al. (1996), which is known to produce surface fluxes that are in better agreement with observations. In these adjusted NCEP fluxes the global mean sensible and latent heat fluxes are reduced, especially in the western boundary currents and the high latitude marginal seas. The reduction in fluxes is concentrated in the winter period. It must be emphasized that the approach of adjusting the NCEP–NCAR reanalyses surface fluxes used here is less than ideal. It is an offline calculation that ignores the feedbacks between the surface fluxes and the

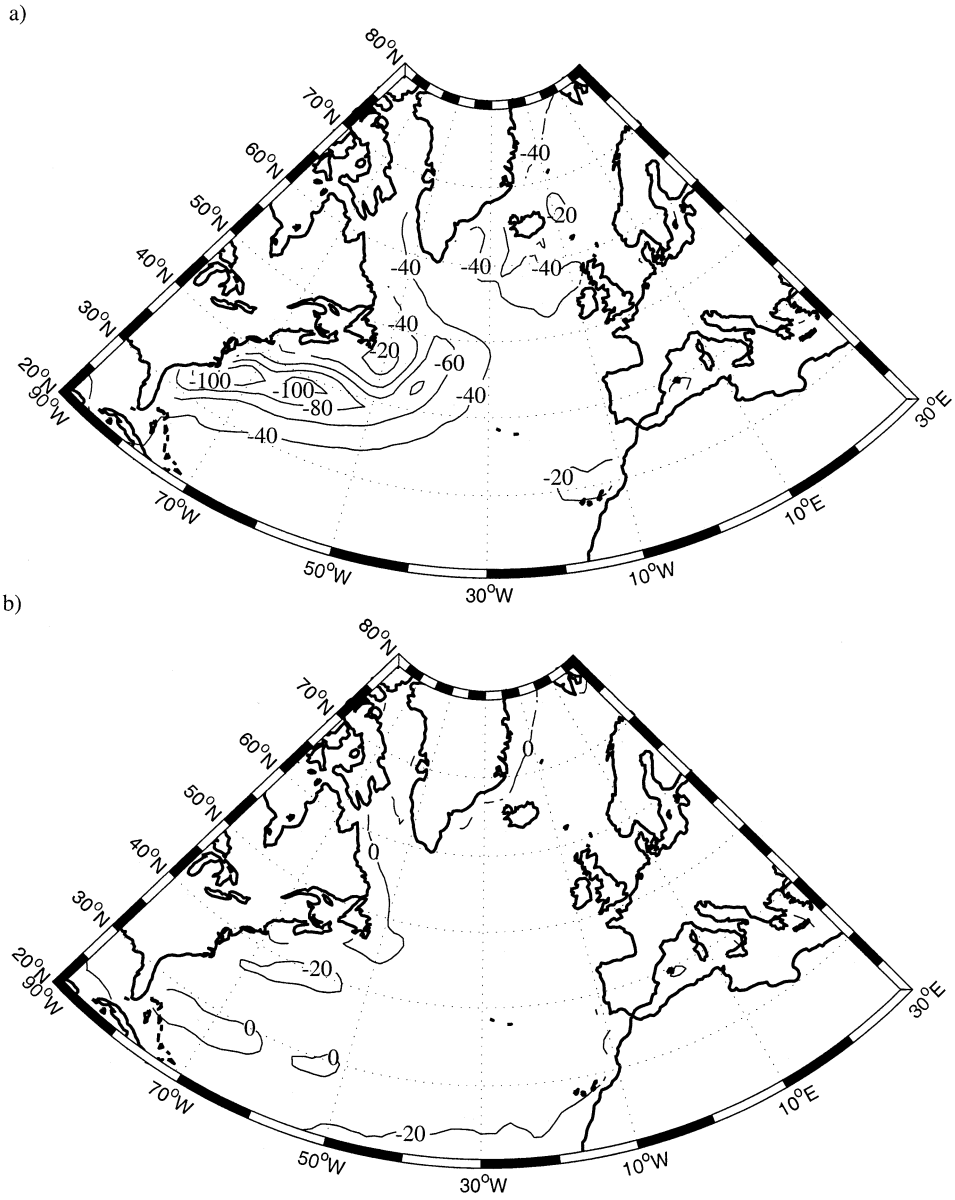

FIG. 16. Difference between the NCEP–NCAR reanalysis latent heat flux and the NCEP-adjusted latent heat flux (W m^{-2}) for (a) winter (DJF) and (b) summer (JJA) over the North Atlantic. Negative values indicate that the latent heat flux from the NCEP–NCAR reanalysis is larger than the corrected value. Climatology based on years 1979–93.

model's atmospheric boundary layer, which would modulate both at each time step. Clearly a more physically sound solution would be the use of a bulk flux algorithm that more closely reflected consensus in the next NCEP–NCAR reanalysis. Note the NCEP operational model moved to such a bulk flux algorithm in 1998—the Zeng et al. (1998) algorithm.

In spite of the fact that the NCEP-adjusted fluxes are in better agreement with observations, there still exists considerable disagreement with other recent climatologies over the western boundary currents. These differences are due to different surface layer meteorological input data, bulk flux algorithms, data sampling, and analysis procedures. At this stage we would suggest that it is not possible to determine which of the climatologies are most accurate. However, we would point out that the NCEP-adjusted fluxes are generally more in line with the in situ climatologies than the raw reanalysis products from NCEP–NCAR. This study serves to illustrate the point that accurate regional assessments are a key step to accurate global assessments. A corollary to this finding is that further field work in critical areas, such as the western boundary currents and the high latitude marginal seas, is essential to improving our un-

derstanding of air–sea interaction at both regional and global scales.

Acknowledgments. The NCEP–NCAR reanalysis data was provided by the NOAA Climate Diagnostics Center. We would like to acknowledge the cooperation of Drs. Xue and Blanton in accessing the GALE IOP2 data. The buoy data used in this paper were provided by the NOAA National Data Buoy Center. The ERA-15 climatology was kindly provided by Dr. Barnier. The SOC climatology was kindly provided by Dr. Josey. We thank the reviewers for their suggestions.

REFERENCES

Agee, E. M., and R. P. Howley, 1977: Latent and sensible heat flux calculations at the air–sea interface during AMTEX 74. *J. Appl. Meteor.,* **16,** 443–447.

Blanton, J. O., J. A. Amft, D. K. Lee, and A. Riordan, 1989: Wind stress and heat fluxes observed during winter and spring, 1986. *J. Geophys. Res.,* **94,** 10 686–10 698.

Bony, S., Y. Sud, K. M. Lau, J. Susskind, and S. Saha, 1997: Comparison and satellite assessment of NASA/DAO and NCEP–NCAR reanalyses over tropical ocean: Atmospheric hydrology and radiation. *J. Climate,* **10,** 1441–1462.

Brown, R. A., 1990: Surface fluxes and remote sensing of air–sea interactions. *Current Theory,* G. L. Geernaert and V. J. Plant, Eds., Vol. 1, *Surface Waves and Fluxes,* Kluwer Academic, 7–27.

Bumke, K., U. Karger, and K. Uhlig, 2002: Measurements of turbulent fluxes of momentum and sensible heat over the Labrador Sea. *J. Phys. Oceanogr.,* **32,** 410–410.

Bunker, A. F., and L. V. Worthington, 1976: Energy exchange charts of the North Atlantic Ocean. *Bull. Amer. Meteor. Soc.,* **57,** 670–678.

Businger, J. A., J. C. Wyngaard, Y. Izumi, and E. F. Bradley, 1971: Flux-profile relationships in the atmospheric surface layer. *J. Atmos. Sci.,* **28,** 181–189.

da Silva, A. M., C. C. Young, and S. Levitus, 1994: *Algorithms and Procedures.* Vol. 1, *Atlas of Surface Marine Data 1994,* NOAA Atlas NESDIS 7, 416 pp.

DeCosmo, J., K. B. Katsaros, S. D. Smith, R. J. Anderson, W. A. Oost, K. Bumke, and H. Chadwick, 1996: Air–sea exchange of water vapor and sensible heat: The Humidity Exchange Over the Sea (HEXOS) results. *J. Geophys. Res.,* **101,** 12 001–12 016.

Dyer, A. J., 1974: A review of flux-profile relationships. *Bound.-Layer Meteor.,* **7,** 363–372.

Fairall, C. W., E. F. Bradley, D. P. Rogers, J. B. Edson, and G. S. Young, 1996: Bulk parameterization of air–sea fluxes for the Tropical Ocean–Global Atmosphere Coupled Ocean–Atmosphere Response Experiment. *J. Geophys. Res.,* **101,** 3747–3764.

Garnier, E., B. Barnier, L. Siefridt, and K. Béranger, 2000: Investigating the 15 year air–sea flux climatology from the ECMWF reanalysis project as a surface boundary condition for ocean models. *Int. J. Climatol.,* **20,** 1653–1673.

Garratt, J. R., 1992: *The Atmospheric Boundary Layer*. Cambridge University Press, 316 pp.

Grachev, A. A., C. W. Fairall, and S. E. Larsen, 1998: On the determination of the neutral drag coefficient in the convective boundary layer. *Bound.-Layer Meteor.,* **86,** 257–278.

Grossman, R. L., and A. K. Betts, 1990: Air–sea interaction during an extreme cold air outbreak from the eastern coast of the United States. *Mon. Wea. Rev.,* **118,** 324–342.

Hines, K. M., D. H. Bromwich, and G. J. Marshall, 2000: Artificial surface pressure trends in the NCEP–NCAR reanalysis over the Southern Ocean and Antarctica. *J. Climate,* **13,** 3940–3952.

Holtslag, A. A. M., E. I. F. de Bruijn, and H.-L. Pan, 1990: A high-resolution air mass transformation model for short-range weather forecasting. *Mon. Wea. Rev.,* **118,** 1561–1575.

Josey, S. A., 2001: A comparison of ECMWF, NCEP–NCAR, and SOC surface heat fluxes with moored buoy measurements in the subduction region of the Northeast Atlantic. *J. Climate,* **14,** 1780–1789.

——, E. C. Kent, and P. K. Taylor, 1998: *The Southampton Oceanography Centre (SOC) Ocean–Atmosphere Heat, Momentum and Freshwater Atlas.* Southampton Oceanography Centre Rep. No. 6, Southampton Oceanography Centre, 30 pp.

——, ——, and ——, 1999: New insights into the ocean heat budget closure problem from analysis of the SOC air–sea flux climatology. *J. Climate,* **12,** 2856–2880.

Kader, B. A., and A. M. Yaglom, 1990: Mean fields and fluctuation moments in unstably stratified turbulent boundary layers. *J. Fluid Mech.,* **212,** 637–662.

Kalnay, E., and Coauthors, 1996: The NCEP/NCAR 40-Year Reanalysis Project. *Bull. Amer. Meteor. Soc.,* **77,** 437–471.

Kuo, Y.-H., R. J. Reed, and S. Low-Nam, 1991: Effects of surface energy fluxes during the early development and rapid intensification stages of seven explosive cyclones in the western Atlantic. *Mon. Wea. Rev.,* **119,** 457–476.

Lab Sea Group, 1998: The Labrador Sea Deep Convection Experiment. *Bull. Amer. Meteor. Soc.,* **79,** 2033–2058.

Large, W. G., and S. Pond, 1981: Open ocean momentum flux measurements in moderate to strong winds. *J. Phys. Oceanogr.,* **11,** 324–336.

——, and ——, 1982: Sensible and latent heat flux measurements over the ocean. *J. Phys. Oceanogr.,* **12,** 464–482.

——, J. Morzel, and G. B. Crawford, 1995: Accounting for surface wave distortion of the marine wind profile in low-level ocean storms wind measurements. *J. Phys. Oceanogr.,* **25,** 2959–2971.

Moore, G. W. K., K. Alverson, and I. A. Renfrew, 2002: A reconstruction of the air–sea interaction associated with the Weddell Polynya. *J. Phys. Oceanogr.,* **32,** 1685–1698.

Olson, D. B., 1991: Rings in the ocean. *Annu. Rev. Earth Planet. Sci.,* **91,** 283–311.

Paulson, C. A., 1970: The mathematical representation of wind speed and temperature profiles in the unstable atmospheric surface layer. *J. Appl. Meteor.,* **9,** 857–861.

Raman, S., and A. J. Riordan, 1988: The Genesis of Atlantic Lows Experiment: The planetary-boundary-layer subprogram of GALE. *Bull. Amer. Meteor. Soc.,* **69,** 161–172.

Rasmussen, E. A., 1989: A comparative study of tropical cyclones and polar lows. *Polar and Arctic Lows,* P. F. Twitchell, E. A. Rasmussen, and K. L. Davidson, Eds., A. Deepak Publishing, 47–80.

Renfrew, I. A., and G. W. K. Moore, 1999: An extreme cold air outbreak over the Labrador Sea: Roll vortices and air–sea interaction. *Mon. Wea. Rev.,* **127,** 2379–2394.

——, ——, P. S. Guest, and K. Bumke, 2002: A comparison of surface layer and surface turbulent flux observations over the Labrador Sea with ECMWF analyses and NCEP reanalyses. *J. Phys. Oceanogr,* **32,** 383–400.

Reynolds, R. W., and T. M. Smith, 1994: Improved global sea surface temperature analyses using optimum interpolation. *J. Climate,* **7,** 929–948.

Rogers, W. P., 1986: Presidential commission on the Space Shuttle Challenger accident. [Available online at http://science.ksc.nasa.gov/shuttle/missions/51-1/docs/rogers-commission/table-of-contents.html.]

Schmitz, W. J., and M. S. McCartney, 1993: On the North Atlantic circulation. *Rev. Geophys.,* **31,** 29–49.

Shinoda, T., H. Hendon, and J. Glick, 1999: Intraseasonal surface fluxes in the tropical Western Pacific and Indian Oceans from NCEP reanalyses. *Mon. Wea. Rev.,* **127,** 678–693.

Slutz, R. J., S. J. Lubker, J. D. Hiscox, S. D. Woodruff, R. L. Jenne, D. H. Joseph, P. M. Steurer, and J. D. Elms, 1985: *COADS, Com-*

prehensive Ocean–Atmosphere Data Set, Release 1. Environmental Research Laboratory, Climate Research Program, 262 pp.

Smith, S. D., 1988: Coefficients for sea surface wind stress, heat flux, and wind profiles as a function of wind speed and temperature. *J. Geophys. Res.*, **93,** 15 467–15 472.

Smith, S. R., D. M. Legler, and K. V. Verzone, 2001: Quantifying uncertainties in NCEP reanalyses using high-quality research vessel observations. *J. Climate,* **14,** 4062–4072.

Weller, R. A., M. F. Baumgartner, S. A. Josey, A. S. Fischer, and J. C. Kindle, 1998: Atmospheric forcing in the Arabian Sea during 1994–1995: Observations and comparisons with climatology and models. *Deep-Sea Res.*, **45,** 1961–1999.

WGASF, 2001: Intercomparison and validation of ocean–atmosphere energy flux fields. *Final report of the Joint WCRP/SCOR Working Group on Air–Sea Fluxes*, WCRP Series Rep. No. 112, 296 pp.

Woodruff, S. D., R. J. Slutz, R. L. Jenne, and P. M. Steurer, 1987: A comprehensive ocean–atmosphere dataset. *Bull. Amer. Meteor. Soc.*, **68,** 1239–1250.

Xue, H., J. M. Bane, Jr., and L. M. Goodman, 1995: Modification of the Gulf Stream through strong air–sea interaction in winter: Observations and numerical simulations. *J. Phys. Oceanogr.*, **25,** 533–557.

Zeng, X., M. Zhao, and R. E. Dickinson, 1998: Intercomparison of bulk aerodynamical algorithms for the computation of sea surface fluxes using TOGA COARE and TAO data. *J. Climate,* **11,** 2628–2644.